Molecular Biology of the Cell
Vol. 18, 1143–1152, April 2007

Cornichon-like Protein Facilitates Secretion of HB-EGF and Regulates Proper Development of Cranial Nerves

Hideharu Hoshino,* Tsukasa Uchida,* Toshiaki Otsuki,* Shoko Kawamoto,† Kousaku Okubo,‡ Masatoshi Takeichi,§ and Osamu Chisaka*

*Department of Cell and Developmental Biology, Graduate School of Biostudies, Kyoto University, Kyoto 606-8502, Japan; †Research Information Research Division, National Institute of Informatics, Tokyo 101-8430, Japan; ‡Laboratory for Gene Expression Analysis, Center for Information Biology, National Institute of Genetics, Shizuoka 411-8540, Japan; and §Laboratory for Cell Adhesion and Tissue Patterning, Center for Developmental Biology, RIKEN, Kobe 650-0047, Japan

Submitted August 24, 2006; Revised December 13, 2006; Accepted January 8, 2007
Monitoring Editor: Marianne Bronner-Fraser

During their migration to the periphery, cranial neural crest cells (NCCs) are repulsed by an *ErbB4*-dependent cue(s) in the mesenchyme adjoining rhombomeres (r) 3 and 5, which are segmented hindbrain neuromeres. ErbB4 has many ligands, but which ligand functions in the above system has not yet been clearly determined. Here we found that a *cornichon-like protein/cornichon homolog 2* (*CNIL/CNIH2*) gene was expressed in the developing chick r3 and r5. In a cell culture system, its product facilitated the secretion of heparin-binding epidermal growth factor-like growth factor (HB-EGF), one of the ligands of ErbB4. When CNIL function was perturbed in chick embryos by forced expression of a truncated form of CNIL, the distribution of NCCs was affected, which resulted in abnormal nerve fiber connections among the cranial sensory ganglia. Also, knockdown of *CNIL* or *HB-EGF* with siRNAs yielded a similar phenotype. This phenotype closely resembled that of *ErbB4* knockout mouse embryos. Because HB-EGF was uniformly expressed in the embryonic hindbrain, CNIL seems to confine the site of HB-EGF action to r3 and r5 in concert with ErbB4.

INTRODUCTION

Rhombomeres (r) are segmented structures that transiently appear in the embryonic hindbrain of vertebrates (Lumsden and Krumlauf, 1996). How the neural tube is regionalized and compartmentalized into these cell movement-restricted (Fraser *et al.*, 1990) rhombomeres has gathered many researchers' attention, but the mechanisms involved have still not yet been fully elucidated. Because each rhombomere expresses not only different sets of transcription factors such as Hox genes, but also different sets of secreted signaling molecules, many processes of craniofacial development are dependent on the proper patterning of the hindbrain. One such example is the migration pattern of cranial neural crest cells (NCCs). NCCs are multilineage-potential cells that emigrate from the dorsal edge of the developing neural tube (reviewed by Le Douarin and Kalcheim, 1999). Cranial neural crest cells differentiate into many important cell types such as glia and sensory neurons of the cranial nerves, smooth muscle, connective tissue of the thymus, endothelial cells of the carotid arteries, etc. In the hindbrain region, NCCs do not enter the mesenchyme adjoining odd-numbered rhombomeres, i.e., r3 and r5; and, accordingly, the migration pattern becomes segmented. In avian embryos, this phenomenon is in part dependent on the apoptosis of NCCs in the odd-numbered rhombomeres by BMP4 and MSX2 function under the interactive control of adjacent even-numbered rhombomeres (Graham *et al.*, 1993, 1994). In addition, it has been suggested that the mesenchyme residing around odd-numbered rhombomeres has the property of repulsing the migrating NCCs. Some signal(s) from the neural tube is thought to be the reason for this property. In chicken embryos, the SemaphorinIII/D (formerly collapsin-1)-neuropilin-1 (Nrp1) chemorepellent system is reported to be responsible for the migration-path selection of the trunk and hindbrain NCCs, as was found by use of the stripe-assay and by ectopic expression of Sema3A (Eickholt *et al.*, 1999; Osborne *et al.*, 2005). Another candidate gene that may govern selection of the migration pathway of NCCs is *ErbB4*, a member of the EGF receptor family. *ErbB4* is expressed in r3 and r5, and its knockout (KO) mouse exhibits abnormal NCC migration and axon path finding (Golding *et al.*, 2000). NCCs from r4 of the *ErbB4* KO mouse embryos are able to sense the repulsion signal resident in the mesenchyme adjacent to r3 when grafted into wild-type embryos. On the contrary, wild-type NCCs from r4 migrate into the ErbB4(−/−) mesenchyme located beside r3. These findings indicate that ErbB4 signaling in the r3 instructs the mesenchymal cells surrounding r3 to repulse NCCs. Also, the surface ectoderm around r3 seems to be important for maintaining this repulsion signal (Golding *et al.*, 2004a). *ErbB4* has been shown to be necessary for proper barrier function against cranial NCCs and nerves in the mesenchyme surrounding r3 and r5, although the mechanism establishing the NCC barrier operating in r3 and r5 seems to be slightly different in these areas (e.g., a graft of *ErbB4*-expressing r5 neuroepithelium is not sufficient to induce an NCC-free zone surrounding the r3 area of a recipient) (Golding *et al.*, 2004a). Also in mouse embryos, the NCC-free zone adjacent to r3 is maintained by combinatorial interactions be-

This article was published online ahead of print in *MBC in Press* (http://www.molbiolcell.org/cgi/doi/10.1091/mbc.E06–08–0733) on January 17, 2007.

Address correspondence to: Osamu Chisaka (chisaka@lif.kyoto-u.ac.jp).

tween the r3 neuroepithelium and the adjacent mesenchyme/surface ectoderm (Trainor *et al.*, 2002).

These signaling molecules mentioned above are repeatedly used in many aspects of embryonic morphogenesis; however, the outputs are quite different depending on when and where the signaling takes place. As the activities of these molecules must be tightly regulated, such molecules need to go through many regulatory steps to be secreted. In addition to regulation at transcriptional and translational levels, recent findings have revealed that the activities of some of these molecules are regulated at the transportation and secretion levels. For example, in *Drosophila* development, the activity of Spitz, one of the TGF-alpha homologues, is confined by the activity of the transporter Star and a Golgi apparatus-resident protease known as Rhomboid (Lee *et al.*, 2001; Urban *et al.*, 2002). In this present article we report another example of the regulation of a growth factor at the secretion level.

While searching for genes specifically expressed in the embryonic hindbrain/pharyngeal area, we found the *CNIL* gene to be transiently expressed in a restricted manner, i.e., only in r3 and r5. *CNIL* is one of the homologues of the *Drosophila* gene *cornichon* (*cni*), which is necessary for the transportation of Gurken (one of the TGF-alpha homologues) to a transitional endoplasmic reticulum (tER) site (Herpers and Rabouille, 2004) and promotes the incorporation of Gurken into coat protein complex II (COPII) vesicles (Boekel *et al.*, 2006). Another important piece of information has come from the study of Erv14p, the yeast homolog of CNIL. Erv14p of budding yeast interacts with COPII components and is localized in the ER and Golgi membranes. Mutation of the COPII-binding site (carboxyl-terminus domain) of Erv14p causes the accumulation of the transmembrane protein Axl2p in the ER and thus a lack of Axl2p protein localization to the nascent bud tips or to the mother bud site (Powers and Barlowe, 2002). Likewise, we found that when *CNIL* function was suppressed by introducing a plasmid designed to express the carboxyl-terminus–deleted form (ΔC) of CNIL, the distribution of cranial NCCs was perturbed, and resulted in a cranial nerve-misrouted phenotype quite resembling that of the *ErbB4* KO mouse embryo. ErbB4 is known to bind many EGF motif–containing molecules such as HB-EGF, betacellulin (BTC), epiregulin (EREG), and neuregulins (Nrg1, 2, 3, 4; reviewed in Olayioye *et al.*, 2000; Carpenter, 2003). Because *Drosophila* Cornichon (Roth *et al.*, 1995) is known to be a transporter of Gurken (TGF-alpha homolog), in this study we searched for EGF motif–containing protein transported by CNIL. Among known ErbB4 ligands, we found that HB-EGF bound CNIL and was efficiently secreted into the culture medium when both molecules were coexpressed in cultured cells. Because HB-EGF expression is ubiquitous in the developing hindbrain, CNIL seems to restrict HB-EGF/ErbB4 signaling to r3 and r5 by its specific expression in these rhombomeres. Because signaling transmitted by ErbB receptors is involved in many aspects of embryonic development, these findings may better explain the precise spatial and temporal pattern of ErbB receptor activation during embryonic development.

MATERIALS AND METHODS

Animals

Fertilized hen eggs from Yamagishi Farm (Kyoto, Japan) were incubated at 38.5°C in a humidified environment to the stages required (Hamburger and Hamilton, 1951).

Antibodies

Rabbit anti-CNIL antibody was raised against a peptide (GNPARARERLKNIERIC) that is a part of chicken CNIL. For production of the rat anti-chicken HB-EGF antibody, the protein directed by the N-terminally 6xhistidine-tagged whole ORF was synthesized in *Escherichia coli* by using the pColdI vector (Takara, Tokyo, Japan).

Cloning of Chicken CNIL cDNA

A 186-base pair fragment of *CNIL* cDNA was amplified from a st-17/18 chicken embryo cDNA library by degenerate PCR using the primers recognizing sites where mouse cni and cnil amino acid sequences were conserved. The sequences of the primers were 5′-TTYGCNGCNTTYTGYTAYATG-3′ and 5′-CCAYTCNGCNGCRCANARRAACAT-3′. The cDNA library was then screened with the fragment thus generated as a probe, after which 5′-RACE was performed to obtain the entire ORF.

Homology alignment was carried out with the ClustalW (European Molecular Bioinformatics Institute, http://www.ebi.ac.uk/clustalw/) computer program. The putative transmembrane regions were deduced by the use of SMART software (http://smart.embl-heidelberg.de/).

In situ Hybridization

Whole-mount in situ hybridization was performed as described earlier (Watari *et al.*, 2001). Digoxigenin-labeled RNA probes were used at 0.5 μg/ml for the *SOX10* probe and at 0.1 μg/ml for the chicken *CNIL* probe (0.8-kb cDNA fragment covering nearly the entire ORF). For transcription of the chicken *SOX10* antisense riboprobe, a cDNA fragment amplified by RT-PCR with the following primers was used: 5′-AATGGCACTTGCCTGAGCACCTC-3′ and 5′-CTCCGTGGCTGGTACTTGTAGTC-3′.

Construction of Vectors

Expression vectors were constructed by using either a modified pCApA vector (Niwa *et al.*, 1991) or pcDNA3.1/Myc-His(+)A (Invitrogen, Carlsbad, CA). For some vectors, a C-terminal FLAG epitope (Hopp *et al.*, 1988) or enhanced green fluorescent protein (eGFP) was added as a tag. A C-terminus deletion of CNIL was introduced by PCR. ARIA (NRG1), was cloned by RT-PCR with 5′-GATATCATGTGGGCCACCTCTGAAGG-3′ and 5′-GTCGACTTATACAGCAATAGGGTCTT-3′ as primers, and then the HA epitope was added as described earlier (Wang *et al.*, 2001). The cDNA of Rat NTAK (NRG2) cDNA was kindly donated by S. Higashiyama. To make an expression vector of the secreted form of HB-EGF, sHB-EGF, we inserted a stop codon after the 152nd codon. To make sARIA-HA and sNTAK-3*FLAG, we amplified each cDNA fragment by using primer set (5′-GAATTCAATGTGGGCCACCTCTGAAGG-3′/5′-TCTAGATTAGAAGCTGGCCATTACGTAGT-3′)and (5′-GAATTCAATGCGGCAGGTTTGCTGCTC-3′/5′-CTCGAGCTTCTGGTACAGCTCCTCAG-3′), respectively. Then these fragments were subcloned into the p3XFLAG CMV13 (Sigma, St. Louis, MO). An ErbB4-eGFP expression plasmid was constructed by inserting human ErbB4 cDNA (a gift from N. E. Hynes) into pCApA vector together with an eGFP cassette for a C-terminal tag.

In Ovo Electroporation

In ovo electroporation of st-9 embryos was performed as described previously (Kubo *et al.*, 2003). DNA solution (pCA-CNIL or pCA-ΔC-CNIL: 7.5 mg/ml, pCAGAP-eGFP:1.6 mg/ml, and 0.05% W/V fast green) was injected into the lumen of the hindbrain. pCAGAP-eGFP drives the expression of eGFP (Ichii, unpublished results). The anode was placed just beside the hindbrain, and a cathode-tungsten microelectrode was inserted into the lumen of the hindbrain. Electric pulses were applied for 25 ms, three times, each at 7 V. The embryos were allowed to develop at 38.5°C up to the desired stage and processed for further experiments. For rescue experiments, pCA-sHB-EGF, p3XFLAG CMV13-sARIA-HA or p3XFLAG-CMV13-sNTAK was also added (sHB-EGF and sNTAK-3XFLAG at 8.4 mg/ml and sARIA-HA at 7.5 mg/ml).

CNIL Knockdown with Small Interfering RNA

For RNA interference (RNAi) of the *CNIL* gene in the chick developing hindbrain, 25 mer double-stranded RNAs (60 μM, Stealth RNAi; Invitrogen) were electroporated into the hindbrain of st-9 chick embryos. The target sequences of the small interfering RNAs (siRNAs) were as follows: CNIL 715, 5′ CGCCATCCCTATGCGGCTCAATAAA 3′; CNIL 87, 5′ CATCTGGCATATCATCGCTTTCGAT 3′; CNIL 236, 5′ TCCATGGGCTCTTCTGTCTGATGTT 3′; HB-EGF 447, 5′ CATCCTGCATATGCCAGCCAGGATA 3′; HB-EGF 461, 5′ CAGCCAGGATATCATGGAGAGAGAT 3′; and HB-EGF 567, 5′ TGTCCTCTCTGTGCCTTGTCATCAT 3′. The numbers indicate the start nucleotide positions in the genes (CNIL; GenBank Accession number AB232677, HB-EGF; AF131224). Medium GC-content control RNA (Invitrogen) was used for the negative control. The effectiveness of siRNAs was confirmed by transfecting HEK-293T cells with siRNA, and the protein produced by CNIL or HB-EGF expression plasmids was detected by Western blotting with anti-CNIL or anti-HB-EGF antibody. The concentration of the siRNAs was 60 μM in distilled water. The electroporation conditions were the same as for the other expression plasmid DNAs.

Whole-Mount Immunostaining of Chicken Embryos

Whole-mount immunostaining of st-19/20 embryos was performed as described previously (Davis *et al.*, 1991) with mAb specific for chicken neurofilaments

(Hatta *et al.*, 1987). HRP-conjugated anti-mouse IgG (1:200; GE Healthcare, Chalfont St. Giles, United Kingdom) was used for the secondary antibody; and diaminobenzidine (1 mg/ml in PBST, Sigma), as the colorimetric substrate. Some embryos were dehydrated with methanol and cleared in benzylalcohol-benzylbenzoate (1:2).

Immunohistochemistry

St-12-13 embryos were sectioned at 20 μm and then treated with rat anti-cHB-EGF overnight at 4°C. After having been washed with PBS, the sections were treated with Alexa Fluor 488 goat anti-rat IgG (1:200; Molecular Probes, Eugene, OR) and Alexa Fluor 568 phalloidin (Molecular Probes). The samples were mounted by using FluorSave Reagent (Calbiochem, La Jolla, CA).

Cell Culture

Human embryonic kidney derived HEK-293 and HEK-293T cells were cultured in a 1:1 mixture of DMEM and Ham's F12 medium supplemented with 10% fetal bovine serum.

To establish ErbB4-eGFP stable transfectants (HEK-293::ErbB4-eGFP), we transfected HEK-293 cells with pCAErbB4-eGFP vector and pPGK-Puro by using Effectine Transfection Reagent (QIAGEN, Santa Clarita, CA) according to the manufacturer's protocol and then subsequently selected with puromycin.

Activation of ErbB4 by sHB-EGF, sARIA (sNRG1), or sNTAK (sNrg2)

HEK-293T cells were transfected with sHB-EGF, sARIA, or sNTAK expression vectors. After 24 h, the medium was changed to that without serum, and the cells were incubated for another 24 h. Each conditioned medium was centrifuged at 6000 $\times$ *g* relative centrifugal force to remove floating cells. HEK-293::ErbB4-eGFP cells starved overnight in medium without serum were incubated in these conditioned media for 5 min and then immediately lysed with Laemmli's sample buffer (Laemmli, 1970).

Coimmunoprecipitation

HEK-293T cells cultured in 10-cm dishes were transfected with 2 μg plasmid DNA of each construct. After 36 h of incubation, the cells were pelleted and lysed with 0.1% Triton X-100 in TBS. FLAG or eGFP fusion proteins were immunoprecipitated with the respective anti-FLAG M2 (Sigma) or rabbit anti-GFP antibody (Molecular Probes). The immunoprecipitates were dissolved in Laemmli's sample buffer and boiled for 5 min.

Cell-Surface Biotinylation

Biotinylation of the cell surface was performed as described previously (Gechtman *et al.*, 1999). HEK293T cells were transfected with pcDNA3.1 cHB-EGF-eGFP and pcDNA3.1 CNIL, pcDNA3.1ΔC-CNIL or pcDNA3.1/Myc-His(+)A vectors at a ratio of 1:3. After 36 h, the cells were washed with ice-chilled 1 mM Ca^{2+}, 1 mM Mg^{2+}/HCMF (HBSS), and subsequently biotinylated by using 0.1 mg/ml EZ-Link Sulfo-NHS-Biotin (Pierce, Rockford, IL) in HBSS. The reaction was quenched by 1 mM Ca^{2+}, 1 mM Mg^{2+}/TBS. The biotinylation procedure was performed on ice. Cells were lysed by 0.5% Triton X-100, 0.5% NP-40/TBS. cHB-EGF-EGFP was immunoprecipitated by use of mouse anti-GFP (Roche) and protein G Sepharose (GE Healthcare). The immunoprecipitates were dissolved in Laemmli's sample buffer.

Brefeldin A Treatment

HEK-293T cells were transfected with equal amounts of pcDNA3.1cHB-EGF-eGFP and pcDNA3.1CNIL, ΔC-CNIL, or vector without insert. After 10 h of transfection, brefeldin A or the same volume of vehicle (ethanol) was added (20 mg/l) in order to block secretion. The cells were incubated overnight and harvested.

Concentration of sHB-EGF from Conditioned Medium

Equal amounts of pcDNA3.1cHB-EGF and pcDNA3.1CNIL, ΔC-CNIL, or vector without insert were used to transfect HEK-293T cells. After 24 h, the medium was changed to medium without serum, and then the cells were cultured further for 24 h. The conditioned medium was centrifuged at 16,100 rcf for 10 min to remove floating cells, and sHB-EGF was concentrated with a Microcon YM-3 (Millipore, Bedford, MA).

Western Blotting

Antibodies used for Western blotting were the following: rabbit anti-GFP (1:400; Molecular Probes), anti-FLAG M2 (1:200; Sigma), rat anti-cHB-EGF (1:200; this study), rabbit anti-actin (1:800; Sigma), anti-activated MAP kinase (1:1000; Sigma), HRP-conjugated anti-rabbit IgG (1:5000; Jackson ImmunoResearch, West Grove, PA), biotin-conjugated anti-rat IgG (1:1000; GE Healthcare), HRP-conjugated anti-mouse IgG (1:2500; GE Healthcare), HRP-conjugated avidin (1:10,000; Zymed, South San Francisco, CA), and HRP-conjugated anti-rat IgG (1:2000; Jackson ImmunoResearch). Blots were detected with ECL Plus (GE Healthcare).

RESULTS

Cloning and Sequence Analysis of Chicken CNIL cDNA

We have been collecting cDNAs specifically expressed in the mouse embryonic hindbrain. Through this attempt, we found that the *cnil* gene (cDNA sequence in GenBank; Accession number AB006191, also BC059922 under the name of *cornichon-homolog 2*) was expressed in r3 and r5 of 8.5–9.25 embryonic day (E) mouse embryos (Hoshino and Chisaka, unpublished results). Mouse *cnil* is also expressed at the primitive node (E6.5). For analysis of *cnil* function in hindbrain/cranial nerve development, a conditional knockout system using a hindbrain-specific DNA recombinase-expressing transgenic mouse strain would be very useful. However, such a strain (Cre knock-in mouse at *Krox20* loci; Voiculescu *et al.*, 2000) might produce the recombinase at a stage not earlier than the desired stage for the *cnil* gene elimination (*Krox20* transcription starts at nearly the same stage as does that of *cnil*; our unpublished result). Because chicken embryos are easier than mouse ones to manipulate at the embryonic stages of interest, we decided to isolate chicken *CNIL* cDNA for further analysis of this gene function at the stage of hindbrain segmentation. First, we amplified a portion of *CNIL* cDNA from a stage (st) 17–18 (Hamburger and Hamilton, 1951) chick embryo cDNA library with a pair of primers against the conserved region between mouse *cnil* and *cni*. The major PCR product was cloned into a plasmid vector and sequenced. The nucleotide sequence of the amplified cDNA fragment showed high homology, 82%, with mouse *cnil* and had 48-base pair span of nucleotide sequence that was specific to *cnil*. Therefore, we named the cDNA fragment *CNIL*. The entire coding sequence of *CNIL* was obtained by cDNA library screening with the amplified fragment and 5′-RACE. We deposited the *CNIL* cDNA sequence in the GenBank database as Accession number AB232677. The amino acid sequence of CNIL was compared with those sequences of cni and cnil proteins from human and mouse, *Drosophila* cni, and budding yeast homolog Erv14p (Figure 1A). It should be noted that cnil has a stretch of sequences (16 amino acid residues, Nos. 47–62) that is not present in cni. As these cnil-specific sequences are highly conserved among chicken, mouse, and human, this domain may have some important role(s) in the function of these molecules. The cni and cnil proteins have three putative membrane-spanning domains (Figure 1A, indicated in the CNIL sequences with underlines). There are no other marked domains or motifs found in cni or cnil sequences. The carboxy terminus–deleted form (ΔC; truncated at amino acid residue No. 95 at the end of the second transmembrane domain) was constructed for perturbing the CNIL function in the present study. This truncation deletes the suspected COPII-interaction domain (corresponding to amino acid residues 97-101 of the Erv14p, underlined in Figure 1; Powers and Barlowe, 2002), and the resulting product is expected to act as a dominant-negative molecule. Schematic drawing of the protein topology is also shown (Figure 1B).

Expression Pattern of CNIL Gene

To delineate *CNIL* function in the developing chick hindbrain, we first analyzed its expression pattern during embryogenesis from st-9 to st-16 (Figure 2) by in situ hybridization. Expression of *CNIL* transcripts was characterized by their temporally and spatially restricted distribution in r3 and r5. Expression in r3 and r5 started at st-10 and st-11, respectively (Figure 2, B and C), and decreased from st-14 and st-16, respectively (Figure 2, G and H). Faint expression

A

```
                10         20         30         40         50
c-cnil     1 MAFTFAAFCY MLTLVLCASL IFFVIWHIIA FDELRTDFKN PIDQGNPARA      50
m-cnil     1 MAFTFAAFCY MLTLVLCASL IFFVIWHIIA FDELRTDFKN PIDQGNPARA      50
h-cnil     1 MAFTFAAFCY MLTLVLCASL IFFVIWHIIA FDELRTDFKN PIDQGNPARA      50
m-cni      1 MAFTFAAFCY MLALLLTAAL IFFAIWHIIA FDELKTDYKN PIDQCN----      50
h-cni      1 MAFTFAAFCY MLALLLTAAL IFFAIWHIIA FDELKTDYKN PIDQCN----      50
d-cni      1 MAFNFTAFTY IVALIGDAFL IFFAIFHVIA FDELKTDYKN PIDQCN----      50
Erv14p     1 ----MGAWLF ILAVVVNCIN LFGQVHFTIL YADLEADYIN PIELCS----      50

               60         70         80         90        100
c-cnil    51 RERLKNIERI CCLLRKLVVP EYCIHGLFCL MFLCAAEWVT LGLNLPLLLY     100
m-cnil    51 RERLKNIERI CCLLRKLVVP EYSIHGLFCL MFLCAAEWVT LGLNIPLLFY     100
h-cnil    51 RERLKNIERI CCLLRKLVVP EYSIHGLFCL MFLCAAEWVT LGLNIPLLFY     100
m-cni     51 ---------- --TLNPLVLP EYLIHAFFCV MFLCAAEWLT LGLNMPLLAY     100
h-cni     51 ---------- --TLNPLVLP EYLIHAFFCV MFLCAAEWLT LGLNMPLLAY     100
d-cni     51 ---------- --SLNPLVLP EYLLHIFLNL LFLFCGEWFS LCINIPLIAY     100
Erv14p    51 ---------- --KVNKLITP EAALHGALSL LFLLNGYWFV FLLNLPVLAY     100

              110        120        130        140        150
c-cnil   101 HLWRYFHRPS DGSEGLFDAV SIMDADILGY CQKEAWCKLA FYLLSFFYYL     150
m-cnil   101 HLWRYFHRPA DGSEVMYDAV SIMNADILNY CQKESWCKLA FYLLSFFYYL     150
h-cnil   101 HLWRYFHRPA DGSEVMYDAV SIMNADILNY CQKESWCKLA FYLLSFFYYL     150
m-cni    101 HIWRYMSRPV MSAPGLYDPT TIMNADILAY CQKEGWCKLA FYLLAFFYYL     150
h-cni    101 HIWRYMSRPV MSGPGLYDPT TIMNADILAY CQKEGWCKLA FYLLAFFYYL     150
d-cni    101 HIWRYKNRPV MSGPGLYDPT TVLKTDTLYR NMREGWIKLA VYLISFFYYI     150
Erv14p   101 NLNKIYN--- --KVQLLDAT EIFRT--LGK HKRESFLKLG FHLLMFFYFL     150

             160
c-cnil   151 YSMVYTLVSF -----
m-cnil   151 YSMVYTLVSF -----
h-cnil   151 YSMVYTLVSF -----
m-cni    151 YGMIYVLVSS -----
h-cni    151 YGMIYVLVSS -----
d-cni    151 YGMVYSLIST -----
Erv14p   151 YRMIMALIAE SGDDF
```

B

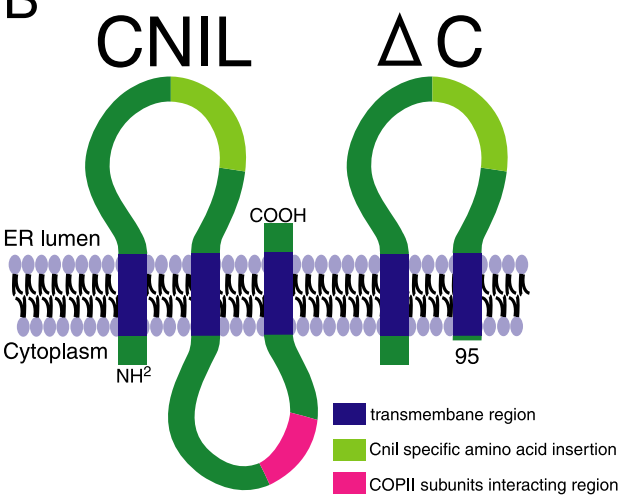

Figure 1. (A) Predicted protein-sequence alignment of chicken CNIL (c-cnil), mouse cnil (m-cnil), human CNIL (h-CNIL), mouse Cornichon (m-cni), human CORNICHON (h-cni), *Drosophila* cornichon (d-cni), and budding yeast Erv14p. For maximum matching, gaps were introduced among the sequences. The residues are shaded when they are identical to those conserved among cnil sequences. The residues in red are conserved among all the cnil family member proteins including Erv14p. The underlined sequences of chicken CNIL indicate the putative transmembrane domains. Also, the underlined part of the Erv14p sequence indicates the COPII interaction domain. Note that cnil sequences have a specific insert of 16 residues at residues 47–62. The truncation point for creating the carboxy-terminus–deleted form (ΔC-CNIL) is between the 95th and 96th residue of chicken CNIL. (B) Schematic drawing of the topology of wild-type CNIL and ΔC-CNIL.

was also detected in NCCs that had migrated out from r5 (arrowhead in Figure 2F indicates NCCs from r5). Longitudinally half-cut st-12 embryo specimens were individually hybridized with the *Hoxb1* or *CNIL* probe (Figure 2I). In the st-12 neural tube, *Hoxb1* was expressed in r4 and from r7 to the caudal part of the spinal cord. Lateral views of the embryo show that *CNIL* was expressed in r3 and r5. Sectioning the stained embryos revealed a dorsoventral distribution of the mRNA. The dorsal one-fourth of the neural tube showed strong expression of CNIL (Figure 2J). At this moment, *CNIL* expression other than in the hindbrain area has not been extensively characterized. The detailed analysis of mouse *cnil* and chicken *CNIL* expression in other organs will be described elsewhere.

Cranial Nerve Defects Resulting from Introduction of the Truncated CNIL into Chicken Embryonic Hindbrain

To elucidate the function of *CNIL* in the development of the hindbrain and its derivatives, we constructed a Δ*C-CNIL* expression plasmid and introduced it into the st-9 chick embryonic hindbrain (r3 to r5) by in ovo electroporation. Positions of the exogenous gene expression were monitored by viewing the fluorescence of eGFP (enhanced green fluorescent protein) from a coelectroporated expression vector (Figure 3E). The injection points were mainly in r3-r5. This ΔC-CNIL was expected to act as a dominant-negative molecule, because it lacked the putative COPII-binding domain. This strategy was adopted from a similar experiment on the

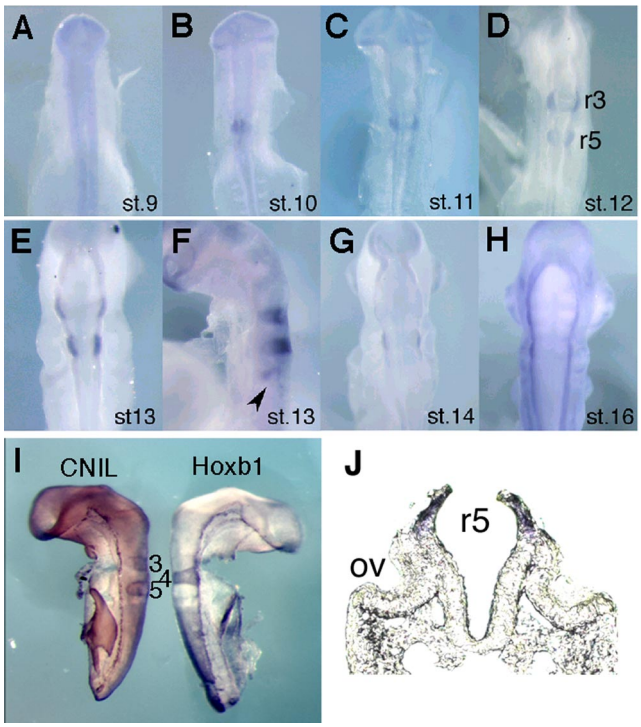

Figure 2. Expression pattern of chicken *CNIL* during rhombomere formation. (A–H) In situ hybridization of chicken embryos for *CNIL* mRNA at st-9 to st-16. Dorsal views with rostral side at the top except for F (lateral view) are presented. (B) At st-10, *CNIL* expression starts in primordial rhombomere (r) 3. (D) At st-12, *CNIL* expression is observed in both r3 and r5 cells. (E and F) The *CNIL* expression level is high at the dorsal edge of the neural tube and at the alar plate at st-13. Arrowhead in F indicates the expression in the NCCs arising from r5. (G and H) At st-14-16, gradually *CNIL* expression decreases and fades out. (I) At st-13, an embryo was longitudinally cut, and each fragment was hybridized with either *CNIL* or *Hoxb1* probe. Numbers beside the hindbrain area indicate the respective rhombomeres. (J) This cross section of a st-13 embryo at r5 level shows that *CNIL* expression is high at the alar plate. ov, otic vesicle.

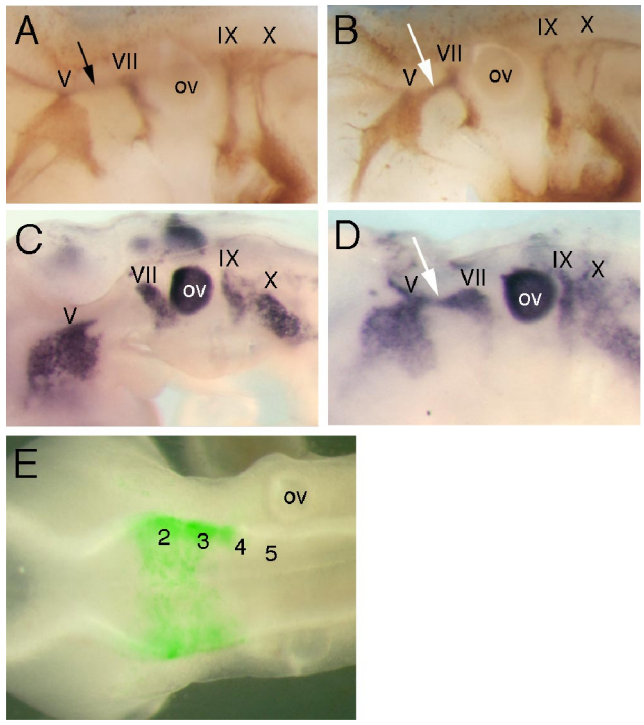

Figure 3. Projection of the cranial nerves and distribution of the NCCs are affected by ΔC-CNIL. (A and B) Whole-mount immunostaining with anti-neurofilament mAb of control (A, eGFP expression plasmid-electroporated) and ΔC-CNIL expression vector-electroporated (B) embryos at st-9. V, trigeminal nerve; VII, facial nerve; IX, glossopharyngeal nerve; X, vagus nerve; ov, otic vesicle. (C and D) Whole-mount in situ hybridization for *SOX10* (glial lineage NCC marker) of st-17 control (C) and ΔC-*CNIL* expression vector-electroporated (D) embryos. Black arrow in A indicates spinal tracts in the neural tube. White arrows in B and D indicate abnormal axon bundles (not in the neural tube) and NCC distribution between the Vth and VIIth ganglia, respectively. Note that these abnormal axon bundles are located more lateral to the entry/exit points of the Vth and VIIth nerves. (E) Dorsal view of a representative specimen with green eGFP signals (pseudocolored) shows the area where expression vectors were introduced by in ovo electroporation. Arabic numerals indicate corresponding rhombomeres.

yeast *cnil* homolog *Erv14p*; i.e., when amino-acid numbers 97-101 of the Erv14p were replaced with alanines, COPII-binding competence was abolished (Powers and Barlowe, 1998, 2002). The stage at electroporation (st-9) is just when NCCs start their emigration from the hindbrain. Δ*C-CNIL* expression plasmids were introduced at st-9, and the embryos were then examined at st-20 for cranial nerve formation. Abnormal axonal projection of the trigeminal (Vth cranial nerve) and facial (VIIth) nerves was observed after immunohistochemical staining for neurofilaments (Figure 3B). The frequency of such abnormalities observed as a consequence of the ΔC-CNIL action was 17/36. Less frequently (9/30), the same phenotype was observed by overexpression of the wild-type *CNIL*. The introduction of the control *eGFP* expression vector yielded the abnormal phenotype at a much lower frequency (4/33). The frequency of the above phenotype was very significantly higher when Δ*C-CNIL* was introduced into the chick embryonic hindbrain than when the control eGFP was used for the transfection ($p = 0.00167$; Mann-Whitney *U* test). The p values of wild-type *CNIL* versus *eGFP* and Δ*C-CNIL* versus wild-type were 0.0823 and 0.15708, respectively (not statistically significant). When Δ*C-CNIL* was introduced into the r3-r5 neuroepithelium, there appeared abnormal nerve connections between the Vth and VIIth ganglia (Figure 3B). The phenotype was further characterized by whole-mount in situ hybridization with the chicken *SOX10* anti-sense RNA probe, which detects the migrating NCCs of the glial lineage (Kuhlbrodt *et al.*, 1998; Figure 3, C and D). In the Δ*C-CNIL* expression vector–injected embryos, NCCs were distributed among the mesenchymal cells surrounding r3 of the neural tube, where NCCs usually do not migrate (7/20 embryos). This phenotype was less frequently seen in control GFP expression vector–injected embryos (2/18 embryos). Thus, *CNIL* was shown to play an important role in establishing discrete NCC streams from the hindbrain to the periphery and proper formation of cranial nerves. However, hindbrain segmentation and rhombomere identities were not drastically altered, as judged from the morphologically distinct rhombomeric boundaries, the expression pattern of *Hoxb1* in r4, and the distribution of motor neuron cell bodies (data not shown). Further detailed marker expression analyses may be necessary in a future study.

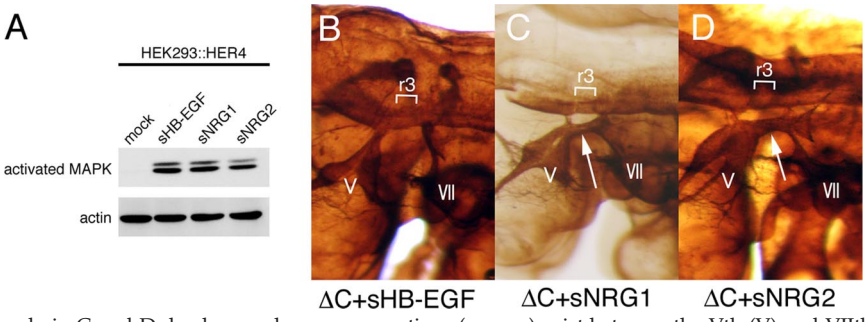

Figure 4. Secreted-form HB-EGF suppresses ΔC-CNIL caused cranial nerve abnormality. (A) The production of biologically active secreted (s) growth factors was confirmed by the detection of activated MAPK after treating HEK-293::HER4(ErbB4) cells with conditioned medium from cultures of sHB-EGF, sNRG1, and sNRG2 expression plasmid-transfected HEK-293T cells. (B–D) ΔC-CNIL and sHB-EGF, ΔC-CNIL and sNRG1, and ΔC-CNIL and sNRG2 expression plasmids, respectively, were electroporated into st-9 chick hindbrains, and nerve fibers were immuno-stained at st-20. Note that only in C and D do abnormal nerve connections (arrows) exist between the Vth (V) and VIIth (VII) ganglia. r3, rhombomere3.

Forced Activation of ErbB4 by a Secreted Form of HB-EGF Can Prevent Cranial Nerve Defects Caused by ΔC-CNIL Transfection

The above-mentioned cranial nerve defects and NCC-distribution phenotypes were very similar to those of *erbB4* KO mice. As mentioned earlier, ErbB4 is known to bind many EGF motif–containing ligands such as HB-EGF, BTC, EREG, and neuregulins (NRG1, 2, 3, and 4). From this information and studies on *Drosophila cni*, we suspected that chicken CNIL carried certain EGF motif–containing protein(s) from the ER to the Golgi apparatus and that its cargo might activate ErbB4.

To examine if forced activation of the ErbB4 signaling pathway could prevent the cranial nerve defects that resulted from the expression of Δ*C-CNIL* in the chicken embryonic hindbrain, we performed coelectroporation of st-9 chicken embryonic neural tubes with the Δ*C-CNIL* expression vector together with one of the expression vectors of the secreted (s) form of known ErbB4 ligands ([HB-EGF, neuregulin-1 [NRG1, ARIA in chicken], and neuregulin-2 [NRG2, NTAK in rat]). The agonistic activities of these proteins were confirmed by downstream MAPK phosphorylation in *ErbB4*-expressing cultured cells (Figure 4A). All the ligands showed similar agonistic activities in this experiment. Because BTC and EREG were not detected in st12-13 chicken embryos, and NRG3 and NRG4 were not detected in E9.0 mouse embryos by RT-PCR, these ligands were not used for this experiment. Embryos after electroporation were collected at st-20, and their cranial nerves were immunostained with an anti-neurofilament antibody. Representative specimens for each combination of the expression vectors are shown in Figure 4, B–D. The frequency of the cranial nerve-defect phenotype was 3/21, 15/19, and 8/20 for ΔC-CNIL + sHB-EGF, ΔC-CNIL + sNRG1, and ΔC-CNIL + sNRG2, respectively. These frequencies were statistically compared with the frequency when only ΔC-CNIL was introduced (17/36, previous section) by using the Mann-Whitney *U* test. The results indicated that only the secreted form of HB-EGF (sHB-EGF) could prevent the cranial nerve defect caused by ΔC-CNIL (Figure 4B; the p value between the ΔC-CNIL vs. ΔC-CNIL + sHB-EGF was 0.00127 <0.05). The introduction of sNRG1 caused a slightly higher frequency of the defect than that of ΔC-CNIL (Figure 4C; $p = 0.0246 < 0.05$). The introduction of sNRG2 apparently did not rescue the embryos from the above phenotype (Figure 4D; $p = 0.6057 > 0.05$). When sHB-EGF, sNRG1 or sNRG2 alone was ectopically expressed, sHB-EGF alone did not cause any abnormality in the cranial nerve development at a statistically high frequency (4/19), but sNRG1 and sNRG2 elicited the abnormal cranial nerve phenotype (15/19 and 8/20, respectively) at frequencies comparable to those with ΔC-CNIL. Because sNRG1 and sNRG2 can bind and stimulate not only ErbB4 but also ErbB2/ErbB3 (required for proper NCCs migration and proliferation, Britsch *et al.*, 1998), overexpression of these ligands would seem to have caused the above cranial nerve phenotype. Also, the phosphorylation pattern of ErbB4 differs after stimulation by NRG1 or by NRG2 (Sweeney *et al.*, 2000). This difference might be one of the reasons why the cranial nerve defect-frequencies differed between sNRG1- and sNRG2-expressing embryos. Altogether, only sHB-EGF could rescue the embryos from the cranial nerve defect caused by ΔC-CNIL.

HB-EGF Is Expressed in the Developing Hindbrain and Interacts with CNIL

Because sHB-EGF could prevent the cranial nerve defects caused by ΔC-CNIL, the HB-EGF expression pattern in the developing hindbrain was examined by immunohistochemical staining using antiserum raised against chicken HB-EGF (Figure 5, A and B). The specificity of the antibody used was confirmed by the colocalized signals of the immunofluorescence and the green fluorescence in the cultured cells expressing HB-EGF-eGFP. In addition, cells that did not express HB-EGF-eGFP were not stained by the antiserum (data not shown). Furthermore, this antiserum stained somites in st-19 chick embryos (data not shown), confirming the similar findings in mouse embryos (Golding *et al.*, 2004b). The staining pattern showed that HB-EGF was expressed ubiquitously in the head region of st-12/13 embryos (Figure 5, A and B). As shown in Figure 5C, this anti-HB-EGF serum could detect HB-EGF protein in the heads (r1 to the 1st somite) of st-12/13 chicken embryo. We then tested whether or not HB-EGF made a complex with CNIL.

The human embryonic kidney cell line HEK-293T was cotransfected with FLAG-tagged CNIL (*CNIL-FLAG*) and eGFP-tagged HB-EGF (*HB-EGF-eGFP*) expression plasmids. The interaction between these two molecules was detected by reciprocal immunoprecipitation using anti-eGFP and anti-FLAG antibodies. As shown in Figure 5D, CNIL and ΔC-CNIL were included in the immunoprecipitates when HB-EGF was specifically immunoprecipitated. Interestingly, ΔC-CNIL precipitated with HB-EGF more efficiently than did the wild type. The reciprocal experiment showed that HB-EGF was efficiently included with the immunoprecipitated ΔC-CNIL (Figure 5E). These data are consistent with the observation made in budding yeast; the precipitation of Axl2 is detected only with COPII binding site–mutated Erv14p. These data together with the information about *Drosophila* cni and yeast homolog protein Erv14p suggest that CNIL could act as a transporter of HB-EGF in r3 and in r5.

Extracellular Secretion of HB-EGF Is Facilitated by CNIL

To analyze the influence of CNIL on the secretion of HB-EGF, we first examined whether the amount of cell-surface HB-EGF was dependent on CNIL. HEK-293T cells were transfected with *HB-EGF-eGFP* and *CNIL* expression plas-

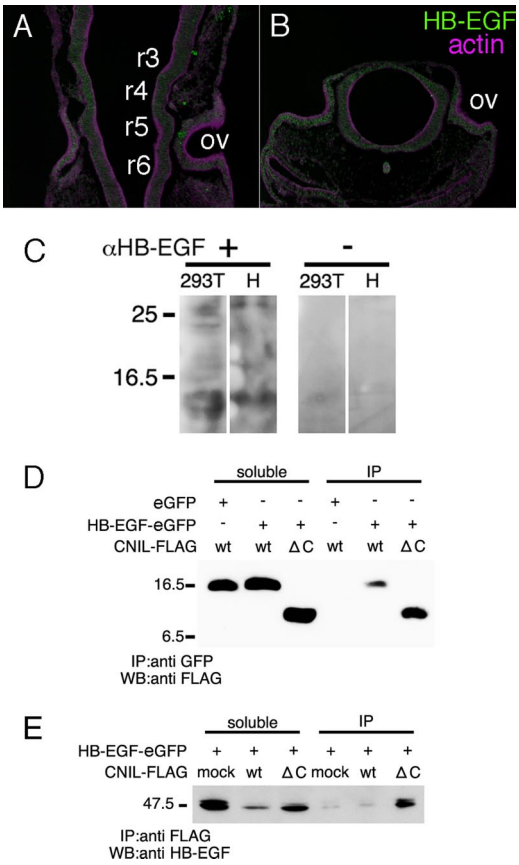

Figure 5. HB-EGF expression and interaction with CNIL protein. (A and B) Immunostaining of coronal (A) and transverse (B) sections of st-12 chick embryos with anti-HB-EGF antibody (green). Actin was also stained (purple) for tissue outlining. HB-EGF is weakly but ubiquitously expressed. r3-6, rhombomeres 3-6; ov, otic vesicle. Pre-immune serum did not give specific signals (data not shown). (C) Immunoblot analysis of st-12/13 chick head extract (H) with anti-HB-EGF antibody (α-HB-EGF). 293T is the control cell extract of HB-EGF expression plasmid-transfected HEK-293T cells. Right panel (−) shows the signals without anti-HB-EGF antibody. (D and E) Reciprocal immunoprecipitation experiments using extracts of HEK-293T cells transfected with HB-EGF-eGFP and the wild-type (WT) or delta-C form (ΔC) of CNIL-FLAG expression plasmids reveal the interaction between HB-EGF and CNIL protein. GFP and FLAG peptide were used as tags. Antibodies used for immunoprecipitation (IP) and detection on the Western blot membranes (WB) are indicated under each panel. Left half of panels ("soluble") shows the amount of CNIL protein (D) or HB-EGF-eGFP protein (E) in the soluble cell extracts. Note that the ΔC-CNIL can interact with HB-EGF more strongly than does the wild type. Also, HB-EGF-eGFP proteins appear as a doublet band due to posttranslational modification.

mid, and then the cell-surface proteins were labeled with biotin. After immunoprecipitation with anti-GFP antibody, cell-surface HB-EGF was detected with HRP-conjugated avidin and a chemiluminescence system. As seen in Figure 6A, the total amount of HB-EGF in the whole cell lysate was reduced by coexpression of CNIL. The ratio of the amount of cell-surface HB-EGF against the total amount of HB-EGF did not differ so much among the samples with or without CNIL or ΔC. This reduction in HB-EGF in the lysate of CNIL-expressing cells might have been caused by promoted secretion of HB-EGF into the culture medium. Actually, this reduction was suppressed by inhibition of vesicle transport from the ER-to-Golgi apparatus by treating cells with brefeldin A (Figure 6B). We next examined whether CNIL facilitated the secretion of HB-EGF into the culture medium. HEK-293T cells were cotransfected with the HB-EGF expression plasmid and the wild-type or Δ*C-CNIL* expression plasmid. After 24 h of incubation, the secreted HB-EGF (sHB-EGF) proteins in the culture media were concentrated with a centrifugal filter device. The specimens were separated on an SDS-PAGE gel, and the HB-EGF was detected with anti-HB-EGF antibody. The results indicated that the wild-type CNIL dramatically enhanced the secretion of the sHB-EGF into the culture medium (Figure 6C). This CNIL-enhanced secretion of HB-EGF well matches the facilitation of budding yeast Axl2p packaging into COPII vesicles in the reconstituted budding reaction by the cnil homolog Erv14p (Powers and Barlowe, 2002). Moreover, the results of the coexpression of both the wild-type CNIL and ΔC-CNIL along with the HB-EGF indicated that ΔC-CNIL acted as a dominant-negative form. ΔC-CNIL suppressed the reduction in HB-EGF from cell lysates caused by wild-type CNIL (Figure 6D), as well as the enhancement of HB-EGF secretion into the culture medium (Figure 6E).

Knockdown of CNIL or HB-EGF with siRNA Causes Cranial Nerve Defects

We next examined if gene knockdown of *CNIL* or *HB-EGF* in the chick hindbrain would cause cranial defects. This experiment should clarify if there exist other genes that have redundant function with *CNIL* or *HB-EGF* in chick hindbrain development. First, the effectiveness of the siRNAs was confirmed by cotransfecting HEK-293T cells with expression vectors of CNIL or HB-EGF and siRNA (Figure 7, A and B). The expression level of *CNIL* and *HB-EGF* was reduced to 18–33% (CNIL) and <5% (HB-EGF) of their control level. Because there was not much difference among the suppression levels with the various siRNAs, we used just one siRNA of *CNIL* (87) and one of *HB-EGF* (447) for in ovo electroporation. The siRNAs of *CNIL* or *HB-EGF* were introduced into the hindbrains of st-9 chick embryos by electroporation. The embryos were collected at st-20 and stained with anti-neurofilament antibody. The results indicate that knockdown of CNIL or HB-EGF resulted in cranial nerve defects similar to those of ΔC-CNIL–expressing embryos (Figure 7, D and E). The frequencies of the above phenotype were 2/18, 9/19, and 7/20 for control siRNA-, *CNIL* siRNA–, and *HB-EGF* siRNA–injected embryos, respectively. These frequencies of abnormality were comparable to that frequency for ΔC-CNIL–expressing embryos. These results support our contention that ΔC-CNIL acts as a dominant-negative molecule and also suggest that CNIL is a main transporter of HB-EGF in the cells of chick embryonic hindbrain and that HB-EGF would be the main agonist of ErbB4.

DISCUSSION

The results in this study are schematically summarized in Figure 8. The *CNIL* gene is expressed in the odd-numbered neuromeres (r3 and r5) of the developing chick hindbrain. In the normal state, HB-EGF is secreted only in r3 and r5, and the activation of ErbB4 leads to the formation of a repulsive barrier in the adjacent mesenchyme. This HB-EGF secretion site-restriction by CNIL may also be important for proper development of the neuromere/pharynegeal tissues other than r3 and r5. When the CNIL activity is perturbed in r3 by a carboxy terminus-deleted form, secretion of HB-EGF is supposedly reduced, as judged from the experiment using cultured cells (Figure 6, C and E). Then the signaling by the

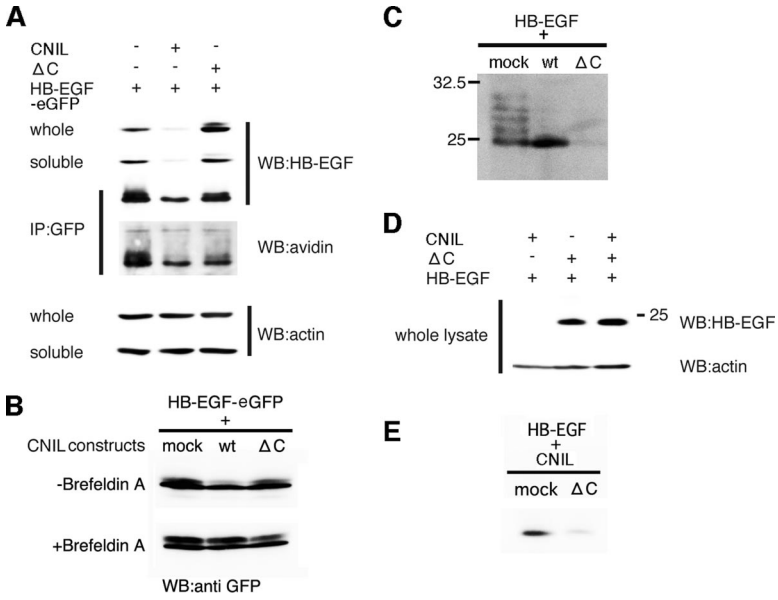

Figure 6. HB-EGF secretion is facilitated by CNIL. (A) Cell-surface HB-EGF was detected by biotinylation. HB-EGF-eGFP and wild-type or ΔC-CNIL expression plasmids were used to cotransfect HEK-293T cells. The biotinylated-HB-EGF-eGFP was detected with HRP-conjugated avidin after immunoprecipitation and SDS-PAGE by using anti-GFP antibody. Total HB-EGF-eGFP in the whole lysates and immunoprecipitates was also detected with anti-HB-EGF antibody. (B) Inhibition of protein transport from the ER to the Golgi apparatus by brefeldin A caused accumulation of HB-EGF-eGFP in wild-type CNIL coexpressing cells. (C) Wild-type CNIL promotes secretion of HB-EGF into the culture medium. HEK-293T cells were transfected with HB-EGF and wild-type CNIL or ΔC-CNIL expression plasmids. Then, secreted HB-EGF from the culture medium was concentrated and detected by immunoblotting. (D) HB-EGF accumulated in ΔC-CNIL, or wild-type CNIL- and ΔC-CNIL–expressing cells. Whole cell lysates were subjected to immunoblotting with anti-HB-EGF antibody. (E) ΔC-CNIL acts as a dominant-negative molecule. HEK-293T cells were transfected with cHB-EGF and wild-type CNIL expression vectors with or without an additional ΔC-CNIL expression or mock plasmid. HB-EGF was quantified as in C. Note that secretion of HB-EGF is reduced in the ΔC-CNIL–expressing cells.

HB-EGF receptor, ErbB4 would be hampered, resulting in reduced NCC-repulsion activity in the mesenchyme lateral to r3. A similar phenotype would be expected for the *CNIL* suppression with siRNA. These phenotypes quite resemble those of the *ErbB4* null mouse embryos (Gassmann *et al.*, 1995) and the dominant-negative *ErbB4* (*DN-HER4*) introduced into chick embryos (Golding *et al.*, 2004a). Although *ErbB4* expression in mouse and chick hindbrains are slightly different, i.e., in dorsal regions of r3 and r5 in the mouse (Gassmann *et al.*, 1995) and in the basal plate in r3 and r5 and at the pial rhombic lip in chick embryos (Dixon and Lumsden, 1999), their functions in selection of the cranial NCC migration path seem to be similar.

ErbB4 is known to bind many EGF motif-containing molecules. From the results of our "rescue" experiment using sHB-EGF, sNRG1, and sNrg2 expression vectors (Figure 4, B–D), the ΔC-CNIL–caused cranial nerve defect seems to have arisen due to faulty HB-EGF secretion. We also showed that CNIL promoted the secretion of HB-EGF from cultured cells into the culture medium. Because the amount of cell-surface HB-EGF was rather reduced in wild-type CNIL-expressing cells, shedding of HB-EGF may also be promoted by CNIL in the cultured cells, although such a function has not been reported to be operative in other organisms. Because the rhombencephalic expression of the proteases involved in HB-EGF shedding was not investigated, whether promoted shedding of HB-EGF, as seen in the cultured cells, also takes place in the chick hindbrain is not known. Anyway, we suspect that CNIL promotes the secretion of HB-EGF in r3 and r5 and that only these rhombomeres receive the HB-EGF stimulus to initiate the repulsion by the mesenchyme. The expression level of HB-EGF in the hindbrain is low, and so far, we have not confirmed any reduction in the HB-EGF secretion in vivo after introduction of ΔC-CNIL. However, our knockdown experiment using siRNA has clearly shown that CNIL and HB-EGF have important roles in cranial nerve development.

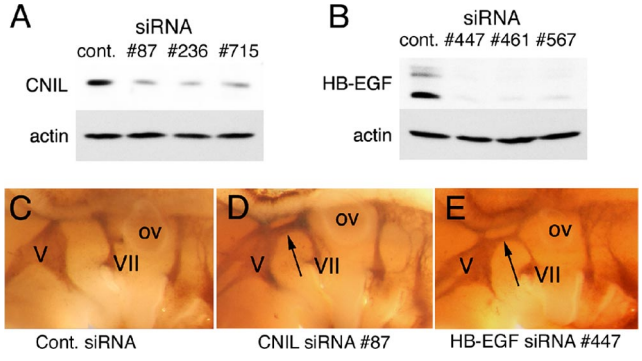

Figure 7. RNAi of CNIL or HB-EGF causes cranial nerve defects. (A) siRNAs suppress CNIL expression from a plasmid vector when cotransfected into HEK293T cells. (B) siRNAs suppress HB-EGF expression. (C–E) Control siRNA- (C), CNIL siRNA- (D), and (E) HB-EGF siRNA-treated chick embryos were stained with anti-neurofilament antibody. The siRNAs were electroporated into st-9 chick hindbrains; and nerve fibers were immunostained at st-20. Note that only in D and E do abnormal nerve connections (arrows) exist between the Vth (V) and VIIth (VII) ganglia. Numbers after siRNAs indicate their nucleotide start positions in the gene.

In the developing vertebrate hindbrain, so far NRG1 has been the only suspected ligand of ErbB4, but our present finding indicates that HB-EGF is another ligand for Erb4 in this area. Knockout mice of *nrg1* also showed cranial nerve defects, but the phenotype is different from that of *ErbB4* KO mice and that of ΔC-CNIL–expressing chick embryos. The proximal ganglia of cranial nerves appeared to be missing in *nrg1* KO mouse embryos, and NCC generation or survival seemed to be dependent on NRG1 protein (Meyer and Birchmeier, 1995). In the mouse hindbrain, the protein encoded by *cnil*, which is expressed in r3 and r5, does not seem to carry Nrg1, because *nrg1* is strongly expressed in r2, 4, and 6, as reported previously (Dixon and Lumsden, 1999). Also, we could not detect any physical interaction between CNIL and NRG1 in coexpressing cells (data not shown). The expression patterns of ErbB4 and NRG1 in the developing hindbrain slightly differ between the chick and mouse. As mentioned above, strong expression domains of ErbB4 and Nrg1 do not overlap in the mouse hindbrain. In the chick hindbrain, the expression domains of ErbB4 and NRG1 partially overlap at the region between the basal plate and the alar plate in r3 of the st-12-13 embryos (Dixon and Lumsden, 1999). At this moment we do

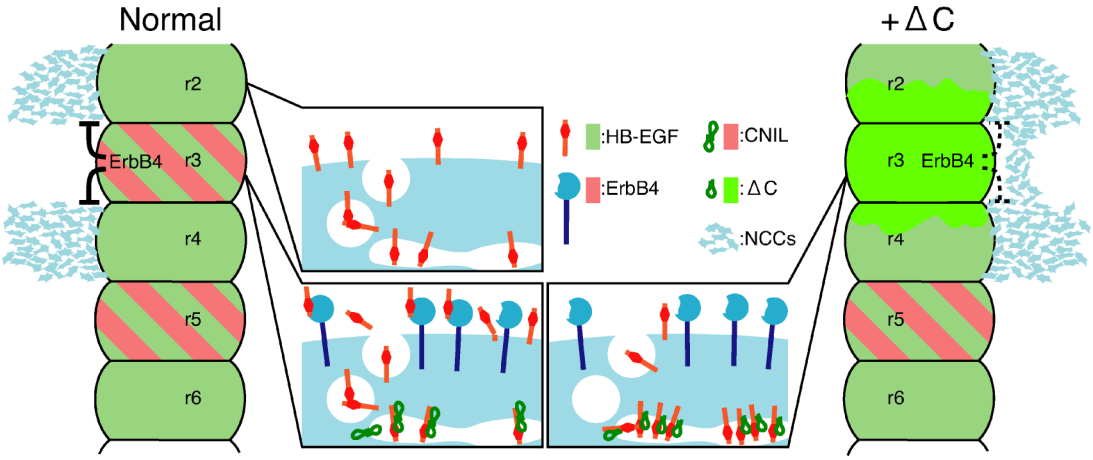

Figure 8. Summary of the CNIL function focusing on r3 of the chick hindbrain. In rhombomeres not expressing CNIL, HB-EGF is not secreted from the cell surface. In normal r3, HB-EGF is efficiently secreted from the cell surface with the aid of CNIL. Subsequently, the mesenchyme adjacent to r3 and r5 inhibits NCC migration into these areas. On the contrary, in ΔC-CNIL–expressing r3, the secretion of HB-EGF is blocked; and NCCs migrate into the mesenchyme beside r3.

not know how this difference between mouse and chicken affects the selection of the NCC migration path.

As was shown in Figure 2, E and 2F, CNIL was expressed in migrating NCCs emigrating from r5. ErbB4 expression in these cells was not observed in the chick hindbrain (Dixon and Lumsden, 1999). At this moment we do not know what ligand-receptor system is supported by CNIL in these cells. Gene expression analysis of these CNIL-positive NCCs and forced expression of ΔC-CNIL in r5-r6 may reveal CNIL function in r5-derived NCCs in the future.

We did not examine presently whether mouse HB-EGF has an expression pattern similar to that of the chicken in the developing hindbrain. Our present study suggests that the secreted form of HB-EGF has an important role in the selection of NCC migration path in the chick hindbrain. There was not much difference in the amount of cell-surface HB-EGF between the in the wild-type CNIL- and ΔC-CNIL–expressing cells. Membrane-bound HB-EGF is known to transmit juxtacrine signals to neighboring cells (Iwamoto and Mekada, 2000). Because HB-EGF KO mice (Iwamoto *et al.*, 2003) and mice in which the HB-EGF locus was replaced with an uncleavable form (HB^{uc}) or a transmembrane domain-truncated form (HB^{Δ}; Yamazaki *et al.*, 2003) have already been generated, examination of the cranial nerve phenotypes of their embryonic hindbrain is anticipated. Such studies should clarify which form of the HB-EGF acts dominantly for the barrier function against NCC migration in mice.

As far as we have checked, we have found no hindbrain segmentation defects or identity alteration of r4; however, there remains a possibility that more detailed analysis using proper markers may reveal some defects in the Δ C-CNIL–expressing neural tube.

There are many mouse gene mutants that show cranial nerve defects, including *COUP-TF1* (Qiu *et al.*, 1997), *Hoxa3* (Manley and Capecchi, 1997; Watari *et al.*, 2001), *ErbB2* (Lee *et al.*, 1995), *ErbB3* (Erickson *et al.*, 1997), *ErbB4* (Gassman *et al.*, 1995), *nrg1* (Meyer and Birchmeier, 1995), *Semaphorin III/D* (*SemaIII*, *collapsin-1*; Taniguchi *et al.*, 1997), *Neuropillin-1* (Kitsukawa *et al.*, 1997), and the *Hes1* and *Hes5* double mutant (Hatakeyama *et al.*, 2006). Among these, *ErbB2*, *ErbB3*, *nrg1* mutants have cranial ganglia of reduced size, suggesting that their products are necessary for the survival of the NCC precursors. But *ErbB4*, *SemaIII*, and *Nrp1* mutants have ganglia of normal size. Recently, the Semaphorin/Neuropilin signaling system in the chick hindbrain was also shown to be necessary for the proper stream-like migration of neural crest cells (Osborne *et al.*, 2005). Signals necessary for the survival or the migration path selection of the NCCs would seem to intermingle with each other. More information is still needed to unravel the complex interactions among different tissues, e.g., hindbrain neural tube, NCCs, ectoderm, and surrounding mesenchyme. Also, the downstream targets of transcription factors whose mutants exhibit cranial nerve defects should be investigated. Studies on the downstream signaling of ErbB4, activated by HB-EGF, would help to identify the molecules responsible for repulsive property of mesenchymal cells adjoining r3.

CNIL is expressed in many tissues, including cancer cells (our unpublished results). Further studies on the CNIL protein should reveal the relationship between cellular behavior and ErbB4 activity in other tissues, which relationship cannot be clarified by just analyzing the expression patterns of ErbB4 and its ligands.

ACKNOWLEDGMENTS

We are grateful to N. Watari-Goshima, Y. Hayakawa, and members of M. Takeichi and T. Uemura's labs for their discussions regarding this study. We thank Drs. K. Umesono and R. Yu for providing the chicken cDNA library, T. Ichii for the modified pCA vectors, N. E. Hynes for ErbB4 cDNA, and S. Higashiyama for NTAK cDNA. This study was supported by grants from the Sumitomo Foundation, the Asahi Glass Foundation, and by a grant-in-aid (18570195) from the Ministry of Education, Science, and the Technology of Japan to O.C.

REFERENCES

Boekel, C., Dass, S., Wilsch-Brauninger, M., and Roth, C. (2006). *Drosophila* Cornichon acts as cargo receptor for ER export of the TGFalpha-like growth factor Gurken. Development *133*, 459–470.

Britsch, S., Li, L., Kirchhoff, S., Theuring, F., Brinkmann, V., Birchmeier, C., and Riethmacher, D. (1998). The ErbB2 and ErbB3 receptors and their ligand, neuregulin-1, are essential for development of the sympathetic nervous system. Genes Dev. *12*, 1825–1836.

Carpenter, G. (2003). ErbB-4: mechanism of action and biology. Exp. Cell Res. *284*, 66–77.

Davis, C. A., Holmyard, D. P., Millen, K. J., and Joyner, A. L. (1991). Examining pattern formation in mouse, chicken and frog embryos with an En-specific antiserum. Development *111*, 287–298.

Dixon, M., and Lumsden, A. (1999). Distribution of neuregulin-1 (nrg1) and erbB4 transcripts in embryonic chick hindbrain. Mol. Cell. Neurosci. *13*, 237–258.

Eickholt, B. J., Mackenzie, S. L., Graham, A., Walsh, F. S., and Doherty, P. (1999). Evidence for collapsin-1 functioning in the control of neural crest migration in both trunk and hindbrain regions. Development *126*, 2181–2189.

Erickson, S. L., O'Shea, K. S., Ghaboosi, N., Loverro, L., Frantz, G., Bauer, M., Lu, L. H., and Moore, M. W. (1997). ErbB3 is required for normal cerebellar and cardiac development: a comparison with ErbB2-and heregulin-deficient mice. Development *124*, 4999–5011.

Fraser, S., Keynes, R., and Lumsden, A. (1990). Segmentation in the chick embryo hindbrain is defined by cell lineage restrictions. Nature *344*, 431–435.

Gassmann, M., Casagranda, F., Oriori, D., Simon, H., Lai, C., Klein, R., and Lemke, G. (1995). Aberrant neural and cardiac development in mice lacking the ErbB4 neuregulin receptor. Nature *378*, 390–394.

Gechtman, Z., Alonso, J. L., Raab, G., Ingber, D. E., and Klagsbrun, M. (1999). The shedding of membrane-anchored heparin-binding epidermal-like growth factor is regulated by the Raf/mitogen-activated protein kinase cascade and by cell adhesion and spreading. J. Biol. Chem. *274*, 28828–28835.

Golding, J. P., Trainor, P., Krumlauf, R., and Gassmann, M. (2000). Defects in pathfinding by cranial neural crest cells in mice lacking the neuregulin receptor ErbB4. Nat. Cell Biol. *2*, 103–109.

Golding, J. P., Sobieszczuk, D., Dixon, M., Coles, E., Christiansen, J., Wilkinson, D., and Gassmann, M. (2004a). Roles of erbB4, rhombomere-specific, and rhombomere-independent cues in maintaining neural crest-free zones in the embryonic head. Dev. Biol. *266*, 361–372.

Golding, J. P., Tsoni, S., Dixon, M., Yee, K. T., Partridge, T. A., Beauchamp, J. R., Gassmann, M., and Zammit, P. S. (2004b). Heparin-binding EGF-like growth factor shows transient left-right asymmetrical expression in mouse myotome pairs. Gene Expr. Pat. *5*, 3–9.

Graham, A., Heyman, I., and Lumsden, A. (1993). Even-numbered rhombomeres control the apoptotic elimination of neural crest cells from odd-numbered rhombomeres in chick hindbrain. Development *119*, 233–245.

Graham, A., Francis-West, P., Brickell, P., and Lumsden, A. (1994). The signaling molecule BMP-4 mediates apoptosis in the rhombencephalic neural crest. Nature *372*, 684–686.

Hamburger, V. G., and Hamilton, H. L. (1951). A series of normal stages in the development of the chick embryo. J. Morphol. *88*, 49–92.

Hatakeyama, J., Sakamoto, S., and Kageyama, Y. (2006). Hes1 and Hes5 regulate the development of the cranial and spinal nerve systems. Dev. Neurosci. *28*, 92–101.

Hatta, K., Takagi, S., Fujisawa, H., and Takeichi, M. (1987). Spatial and temporal expression pattern of N-cadherin cell adhesion molecules correlated with morphogenetic processes of chicken embryos. Dev. Biol. *120*, 215–227.

Herpers, B., and Rabouille, C. (2004). mRNA localization and ER-based protein sorting mechanisms dictate the use of transitional endoplasmic reticulum-Golgi units involved in Gurken transport in *Drosophila* oocytes. Mol. Biol. Cell *15*, 5306–5317.

Hopp, T. P., Prickett, K. S., Price, V. L., Libby, R. T., March, C. J., Cerretti, D. P., Urdal, D. L., and Conlon, P. J. (1988). A short polypeptide marker sequence useful for recombinant protein identification and purification. Biotechnology *6*, 1204–1210.

Iwamoto, R., and Mekada, E. (2000). Heparin-binding EGF-like growth factor: a juxtacrine growth factor. Cytokine Growth Factor Rev. *11*, 335–344.

Iwamoto, R. *et al.* (2003). Heparin-binding EGF-like growth factor and ErbB signaling is essential for heart function. Proc. Natl. Acad. Sci. USA *100*, 3221–3226.

Kitsukawa, T., Shimizu, M., Sanbo, M., Hirata, T., Taniguchi, M., Bekku, Y., Yagi, T., and Fujisawa, H. (1997). Neuropilin-semaphorin III/D-mediated chemorepulsive signals play a crucial role in peripheral nerve projection in mice. Neuron *19*, 995–1005.

Kubo, F., Takeichi, M., and Nakagawa, S. (2003). Wnt2b controls retinal cell differentiation at the ciliary marginal zone. Development *130*, 587–598.

Kuhlbrodt, K., Herbarth, B., Sock, E., Hermans-Borgmeyer, I., and Wegner, M. (1998). Sox10, a novel transcriptional modulator in glial cells. J. Neurosci. *18*, 237–250.

Laemmli, U. K. (1970). Cleavage of structural proteins during the assembly of the head of bacteriophage T4. Nature *227*, 680–685.

Le Douarin, N. M. and Kalcheim, C. (1999). The Neural Crest, 2nd ed., Cambridge University Press.

Lee, K.-F., Simon, H., Chen, H., Bates, B., Hung, M.-C., and Hauser, C. (1995). Requirement for neuregulin receptor erbB2 in neural and cardiac development. Nature *378*, 394–398.

Lee, S., Urban, J. R., and Freeman, M. (2001). *Drosophila* rhomboid-1 defines a family of putative intramembrane serine proteases. Cell *107*, 173–182.

Lumsden, A., and Krumlauf, R. (1996). Patterning of the vertebrate neuraxis. Science *274*, 1109–1115.

Manley, N. R., and Capecchi, M. R. (1997). Hox group 3 paralogous genes act synergistically in the formation of somitic and neural crest-derived structures. Dev. Biol. *192*, 274–288.

Meyer, D., and Birchmeier, C. (1995). Multiple essential functions of neuregulin in development. Nature *378*, 386–390.

Niwa, H., Yamamura, K., and Miyazaki, J. (1991). Efficient selection for high-expression transfectants with a novel eukaryotic vector. Gene *108*, 193–199.

Olayioye, M. A., Neve, R. M., Lane, H. A., and Hynes, N. (2000). The ErbB signaling network: receptor heterodimerization in development and cancer. EMBO J. *19*, 3159–3167.

Osborne, N. J., Begbie, J., Chilton, J. K., Schmidt, H., and Erickholt, B. J. (2005). Semaphorin/Neuropilin signaling influences the positioning of migratory neural crest cells within the hindbrain of the chick. Dev. Dyn. *232*, 939–949.

Powers, J., and Barlowe, C. (1998). Transport of Axl2p depends on Erv14p, an ER-vesicle protein related to the *Drosophila cornichon* gene product. J. Cell Biol. *142*, 1209–1222.

Powers, J., and Barlowe, C. (2002). Erv14p directs a transmembrane secretory protein into COPII-coated transport vesicles. Mol. Biol. Cell *13*, 880–891.

Qiu, Y., Pereira, F. A., DeMayo, F. J., Lydon, J. P., Tsai, S. Y., and Tsai, M. J. (1997). Null mutation of mCOUP-TFI results in defects in morphogenesis of the glossopharyngeal ganglion, axonal projection, and arborization. Genes Dev. *11*, 1925–1937.

Roth, S., Neuman-Silberberg, F. S., Barcelo, G., and Schüpbach, T. (1995). Cornichon and the EGF receptor signaling process are necessary for both anterior-posterior and dorsal-ventral pattern formation in *Drosophila*. Cell *81*, 967–978.

Sweeney, C., Lai, C., Riese, II, D. J., Diamonti, A. J., Cantley, L. C., and Caraway, K. L., III. (2000). Ligand discrimination in signaling through an ErbB4 receptor homodimer. J. Biol. Chem. *275*, 19803–19807.

Taniguchi, M., Yuasa, S., Fujisawa, H., Saga, S., Mishina, M., and Yagi, T. (1997). Disruption of semaphorinIII/D gene causes severe abnormality in peripheral nerve projection. Neuron *19*, 519–530.

Trainor, P., Sobieszczuk, D., Wilkinson, D., and Krumlauf, R. (2002). Signalling between the hindbrain and paraxial tissues dictates neural crest migration pathways. Development *129*, 433–442.

Urban, S., Lee, J. R., and Freeman, M. (2002). A family of Rhomboid intramembrane proteases activates all *Drosophila* membrane-tethered EGF ligands. EMBO J. *21*, 4277–4286.

Voiculescu, O., Charnay, P., and Schneider-Maunoury, S. (2000). Expression pattern of a *Krox-20/Cre* knock-in allele in the developing hindbrain, bones, and peripheral nervous system. Genesis *26*, 123–126.

Wang, J. Y., Miller, S. J., and Falls, D. L. (2001). The N-terminal region of neuregulin isoforms determines the accumulation of cell surface and released neuregulin ectodomain. J. Biol. Chem. *276*, 2841–2851.

Watari, N., Kameda, Y., Takeichi, M., and Chisaka, O. (2001). Hoxa3 regulates integration of glossopharyngeal nerve precursor cells. Dev. Biol. *240*, 15–31.

Yamazaki, S. *et al.* (2003). Mice with defects in HB-EGF ectodomain shedding show severe developmental abnormalities. J. Cell Biol. *163*, 469–475.